

# **Ebola and Marburg virus infection in bats is controlled by a systemic response**

Anitha D. Jayaprakash<sup>a</sup>, Adam J. Ronk<sup>b, c</sup>, Abhishek N. Prasad<sup>b, c</sup>, Michael F. Covington<sup>d</sup>, Kathryn R. Stein<sup>h</sup>, Toni M. Schwarz<sup>g</sup>, Saboor Hekmaty<sup>h</sup>, Karla A. Fenton<sup>c, e</sup>, Thomas W Geisbert<sup>c, e</sup>, Christopher F. Basler<sup>f</sup>, Alexander Bukreyev<sup>b, c, e</sup>, Ravi Sachidanandam<sup>h\*</sup>

**a** Girihlet Inc., Oakland, CA 94609

**b** Department of Pathology, the University Texas Medical Branch, Galveston, Texas, United States of America

**c** Galveston National Laboratory, the University of Texas Medical Branch, Galveston, Texas, United States of America

**d** Amaryllis Nucleics, Oakland, CA 94609

**e** Department Microbiology & Immunology, the University of Texas Medical Branch, Galveston, Texas, United States of America

**f** Center for Microbial Pathogenesis, Institute for Biomedical Sciences, Georgia State University, Atlanta, GA 30303, USA

**g** Department of Microbiology, Mount Sinai School of Medicine, New York, NY 10029

**h** Department of Oncological Sciences, Mount Sinai School of Medicine, New York, NY 10029

\*Ravi Sachidanandam, E-mail: [ravi.mssm@gmail.com](mailto:ravi.mssm@gmail.com)

**Abstract.** The filoviruses Ebola (EBOV) and Marburg (MARV) cause fatal disease in humans and nonhuman primates but are associated with subclinical infections in bats, with *Rousettus aegyptiacus* (Egyptian rousette/ERB) being a natural MARV reservoir. To understand the nature of this resistance, we have analyzed the effects of filovirus infection on the transcriptomes of multiple ERB tissues. We have found that while the primary locus of infection was the liver, transcriptomic changes occurred in multiple tissues, suggesting systemic responses. The transcriptional changes are indicative of inhibition of the complement system, induction of vasodilation, changes in coagulation, modulation of iron regulation, activation of a T cell response, and converting macrophages from the M1 to M2 state. We propose that these events are facets of a systemic anti-inflammatory state that enables effective control of the infection in bats and dissecting this state can inform how to control a filovirus infection in humans.

## Introduction

Ebola (EBOV) and Marburg (MARV) filoviruses cause a severe, frequently fatal disease in humans<sup>1</sup>. For example, the 2004-2005 outbreak of MARV killed 227 out of 252 (90%) infected individuals<sup>2</sup>, while an ongoing EBOV outbreak has killed 2,264 out of 3,444 (66% case fatality)<sup>3</sup>. EBOV and MARV kill by causing a multisystem disease state characterized by hypotension, multisystem organ failure, sepsis-like symptoms, and disseminated intravascular coagulation (DIC) due to profound immune dysregulation, including cytokine storm<sup>4</sup>. Despite the aggressive use of a recently approved Ebola vaccine, control of the ongoing outbreak has been difficult, illustrating an ongoing need to develop our understanding of the pathobiology of these viruses. Remarkably, EBOV and MARV appear to cause no significant disease in their likely (EBOV) or confirmed (MARV) bat reservoirs.

MARV has been isolated from *Rousettus aegyptiacus*, the Egyptian rousette bat (ERB)<sup>5-7</sup>, and ecological and experimental studies have demonstrated that this species serves as a reservoir for the virus<sup>6,8</sup>. Experimental infections of ERBs with MARV have consistently demonstrated that despite viral replication in multiple tissues, animals develop a mostly subclinical disease. This is characterized by mild pathology, such as transient elevation of alanine aminotransferase, elevated lymphocyte and monocyte counts, and some evidence of minimal inflammatory infiltration in the liver<sup>9,10</sup>. Clinical signs of disease are absent<sup>9-13</sup>. Transmission has been demonstrated between co-housed ERBs, and virus is known to be shed in saliva, urine, and feces<sup>8</sup>. However, ERBs do not appear to develop a chronic infection when exposed to MARV, and instead clear the virus and develop at least temporary immunity, including MARV-specific IgG<sup>14</sup>.

Considerable circumstantial evidence suggests that bats are also reservoirs for EBOV<sup>15,16</sup>, including detection of EBOV RNA and anti-EBOV antibodies for multiple bat species. Despite this, infectious EBOV has never been isolated from a wild bat<sup>17</sup>. Although serological surveys have identified antibodies reactive with EBOV antigen in ERBs<sup>18-20</sup>, experimental infection studies performed to date suggest that these animals are refractory to infection<sup>21</sup>, making it very unlikely that they are reservoirs for the virus.

The ability of bats to tolerate viral infections has been a topic of considerable interest, and several models have been proposed to explain this phenomenon. Most of these are centered on the innate immune system, which includes the inflammatory response (induced by cytokines), phagocytosis, natural killer cells, and the complement system. One model posits that bats constitutively express interferons to maintain a basal level of innate immune activity, ready for pathogens to appear<sup>22</sup>, although the universality of this model in bats is questionable<sup>23,24</sup>. An alternative model claims that the resistance is due to a weakened innate immune response, which is attenuated by changes in some proteins such as the stimulator of interferon genes (STING or TMEM173)<sup>25</sup>. However, while this model can explain how viruses can survive in the animal, how the infection is eliminated remains unclear. The similarity of innate immune responses to MARV and EBOV in bat and human cell lines<sup>26</sup> seems to contradict both theories and suggests that the control of viral infections in bats is more complex.

To probe this complexity, we have attempted to test two hypotheses: that the response of bats to filoviruses is systemic, involving multiple interrelated processes, and that the differences in the responses to infection between bats and humans are due to evolutionarily divergent genes. To test these hypotheses, we have analyzed how EBOV and MARV affect global gene expression patterns in various tissues, with a particular focus on evolutionarily divergent genes. Our analysis of these transcriptomes begins to reveal a systemic organismal

response that facilitates the ability of bats to survive filovirus infections and suggest potential therapeutic strategies for controlling human infection.

## RESULTS

### **Inoculation of bats with MARV and EBOV results in detectable viral replication only in some organs**

Eleven ERBs were inoculated subcutaneously with  $10^4$  PFU of MARV or EBOV. Following inoculation, animals were observed at least daily, and bled every other day. Viremia was monitored via ddPCR, and animals were euthanized shortly after becoming viremic. As expected, bats inoculated with MARV or EBOV showed no apparent clinical signs of disease or changes in behavior, with no significant effect on body weight and temperature (**Fig. 1-A, B**). MARV and EBOV were detected by ddRT-PCR in the blood of infected bats, with MARV detected earlier and at a higher copy number than EBOV (**Fig. 1-C**). MARV was detected by plaque assay in livers and spleens of all inoculated animals, and in the salivary glands (2 animals) and kidneys (1 animal) of some animals. (**Fig 1-D**) By contrast, EBOV was only present above the limit of detection in the livers of two inoculated animals and could not be reliably detected elsewhere (**Fig 1-E**).

Two of the three EBOV-inoculated animals presented with histopathological lesions in the liver, consisting of pigmented and unpigmented infiltrates of aggregated mononuclear cells compressing adjacent tissue structures, and eosinophilic nuclear and cytoplasmic inclusions, the changes that were consistent with previous reports<sup>18,21</sup>. In EBOV-infected animals, focal immunostaining with both pan-filovirus and EBOV-VP40 antibodies was observed in the liver of one animal, but very few foci were found, suggesting limited viral replication. MARV-inoculated animals showed histopathology similar to that observed in prior experimental infection studies. Immunohistochemistry with a pan-filovirus antibody suggested that MARV was present in mammary glands and testes, despite the lack of histopathological lesions in these organs. (**Fig 1-F**).

### **MARV and EBOV infection affects the transcriptome of multiple organs**

To examine the response to filovirus infection, we sequenced mRNA from liver, spleen, kidney, lungs, salivary glands, large and small intestine, and testes collected from filovirus inoculated and uninfected bats (**Methods, Table S1**). Consistent with prior reports that liver is the primary target of MARV<sup>27</sup>, and our findings (**Fig. 1, Table S2**), MARV transcripts were most abundant in this tissue (79 transcripts-per-million or tpm), but were also present in spleen (56 tpm), intestine (10 tpm) and lungs(2 tpm) (**Table S2**). EBOV transcripts were detected at very low levels ( $< 1$  tpm) in the livers of inoculated bats and were not detectable in other tissues.

Although viral transcripts were detected primarily in the liver, gene expression patterns were altered in all analyzed tissues, involving thousands of genes, suggesting a systemic response (**Fig. 2**). The changes were highest in the livers of MARV-infected animals, and differed between MARV and EBOV (**Fig. 3, S1**), indicating that the observed changes in gene expression patterns are related to the infectious agent.

### **Evolutionarily divergent bat genes as tools for understanding the response to filovirus infection**

To identify genes that may be relevant to the difference in resistance to filoviruses between humans and bats, we reasoned that homologous genes with greater evolutionary divergence between bats and humans are more likely to diverge in function or regulation as well. This hypothesis made the divergent genes our primary suspects. We also reasoned that focusing first on divergent genes would also simplify the computational analysis of the transcriptomes, further increasing the chance of identifying relevant pathways.

Using this strategy, we first identified a set of 2,439 bat genes that were diverged from their human or mouse homologues according to our criteria (**Fig. 4, Methods**). From this set, we then selected a subset of 264 genes expressed at more than 20 tpm in at least one set of liver samples (MARV, EBOV, or uninfected). Of these 264 genes, the expression of 151 was different in the livers of either MARV or EBOV infected bats relative to uninfected animals (**Fig. 4, Methods**). These 151 genes were then used for the first step of pathway analysis.

The most abundant group in this set comprised genes related to mitochondria (20 genes), followed by genes involved in the vascular system (19), innate immunity (16), tissue regeneration and apoptosis (15), macrophages (13), inflammation (10), metabolism and fatty-acid oxidation (8), T cells (4), complement system (2), digestion (5), and toxin processing (3).

This distribution and available knowledge about the pathways in humans that involve these functions led us focus on the *entire* transcriptomes of the following systems : **i)** innate immune system which includes the inflammatory response, phagocytosis by macrophages, natural killer cells, and the complement system; **ii)** inflammatory response, including acute phase proteins, macrophages activities involving metabolism, fatty-acid oxidation, mitochondrial abundance and function, and tissue regeneration and apoptosis; and **iii)** the vascular system, involving the regulation of blood pressure, coagulation, and iron homeostasis.

### **MARV and EBOV infection induce inflammation, indicated primarily by an acute phase response**

Acute phase proteins (APP) are produced by hepatocytes in the liver in response to inflammatory cytokines, such as Interleukin-1(IL-1), IL-6, and TNF $\alpha$ , and are an important part of the innate immune response<sup>28-30</sup>.

Serum concentration of positive APPs<sup>31</sup>, including SAA1 and SAA2 can dramatically increase (> 10-fold) as a part of the response, while the concentration of negative APPs, including transferrin and albumin, decreases<sup>32</sup>.

We found that MARV, and to a lesser extent EBOV, infection induced APP response in liver, spleen and kidney, with the largest changes in APP expression (>10-fold) observed in the liver (**Table 1, Fig. 5**). However, SAA1 and SAA2 expression also increased to a similar degree in most tissues, not only in the tissues in which the viruses were detected. At the same time, we detected no expression of C-reactive protein (CRP), an APPs used as a marker for measuring inflammation acute-phase-response in humans (**Table 1, Fig. 5**), likely because it is not present in the bats. We conclude bats lack a CRP response, based on not detecting it upon analysis of public mRNA-seq data from infected samples from various species of bats (data not shown). Consistent with the induction of SAA1 and SAA2, we also detected induction of other markers of inflammation including, ORM2, CP, HAMP and the microsomal glutathione S-transferases, MGST1 and MGST2<sup>33</sup> (**Table 1, Fig. 5**).

### **MARV and EBOV infection is associated with an early transition from M1- to M2-dominated populations of macrophages**

Macrophages recognize and phagocytize foreign organisms and damaged host cells, as a part of the innate immune response, and are an important early target for filoviruses<sup>27</sup>. Macrophages can either be in the M1 state, an inflammatory state enabling apoptosis, or in the M2 state, anti-inflammatory state assisting tissue regeneration. A key difference between the M1 and M2 states lies in their metabolism, with the M1 state characterized by hypoxia and glycolysis metabolism<sup>34</sup> and the M2 state is characterized by fatty acid metabolism and abundant mitochondria<sup>35</sup>.

We have found that key markers of the M1 state were upregulated in livers of infected bats (more so in MARV infected animals). These included IRF5, NF- $\kappa$ B, AP1G1 (a subunit of the AP-1 complex), STAT1, and SOCS3

(**Fig. 5, S4, S5**). Likewise, HIF1A<sup>36-38</sup>, which promotes mitophagy and glycolysis metabolism to induce M1 polarization was also upregulated in infected livers, again more so in MARV infection. PKM, which activates HIF1A, and the pyruvate dehydrogenase, PDK1, involved in the response to hypoxia were also upregulated, to a greater degree in MARV than EBOV (**Fig. 5, S4, S5**)<sup>39</sup>.

The M2 state markers, MRC1, arginase-1 (ARG1), IL-10 and TGF- $\beta$ <sup>40</sup>, were highly expressed in livers of bats infected with both viruses (**Fig. 5, S4, S5**), suggesting the presence of M2 macrophages. Several genes related to fatty acid oxidation in M2 macrophages were upregulated by filovirus infection (**Tables S3-8**). CPT2, a gene associated with fatty acid transport was upregulated under filoviral infection (greater in MARV infection). Infected bats also exhibited upregulation of multiple markers of mitochondria abundance another characteristic of M2 macrophages. These included TFAM, OPA1, MFN1/2, and DNMI1L. Two genes involved in mitochondrial biogenesis<sup>41</sup>, HGF-MET and PPARGC1A, are also upregulated upon MARV infection.

Prolonged M1 activity can be harmful to tissues due to their induction of inflammation and apoptosis. This is modulated by a negative feedback system that shifts macrophages from the M1 state to the M2 state<sup>42,43</sup>, controlling inflammation during infection and facilitating the transition to tissue repair and regeneration<sup>44,45</sup>. In our data, the transcriptomes of the MARV-infected liver samples suggest a more equal representation of M1 and M2 macrophages, while in the EBOV-infected liver samples, gene expression suggests an M2-dominated macrophage population, suggesting a conversion from M1 to M2 state is underway over the course of the infection, as the virus is cleared.

The M1 to M2 transition is associated with a change in cellular energy metabolism. GPD2, the mitochondrial glycerol-3-phosphate dehydrogenase, identified as a contributor to the shift in core macrophage metabolism associated with the M1 to M2 transition during infection<sup>46</sup>, was found to be upregulated by filovirus infection (**Fig. 5, S6A**). Inactivating HIF1A also promotes M2 polarization. HIF1AN, the inhibitor of HIF1A, is upregulated in filovirus infected bats. Increased availability of iron also promotes the M1 to M2 polarization shift<sup>47</sup>. Gene expression patterns in EBOV-infected bats, notably ferritin and HBB expression, suggest that iron levels may be elevated in these animals. This supports our other findings of an M2 polarization bias.

### **Expression of key components of the classical complement pathway is inhibited by filovirus infection**

The complement pathway, a part of the immune system, has three branches: the classical pathway, the mannose-binding lectin pathway and the alternative pathway<sup>48</sup>. The classical pathway recognizes antigens bound to antibodies; the lectin pathway binds to sugar molecules on the virus particles, and the alternative pathway is a component of the innate defense against infections.

Several key gene associated with the complement pathway were upregulated by filovirus infection, including C3P1, C4B, C5, C9, C6, and MASP1, while others (C1R, C3, C8G, and MASP2) were downregulated or not expressed (**Fig. 5, S6B**). This indicates that the complement pathway is impacted by filovirus infection in the liver and suggests that aspects of the immune response dependent upon complement such as some forms of antibody-mediated viral neutralization, are compromised.

### **Infected bats exhibit transcriptional signatures of T cell activity**

CD4<sup>+</sup> T cells recognize peptides presented on MHC class II molecules found on antigen presenting cells (APCs) while CD8<sup>+</sup> T cells recognize peptides presented by **MHC Class I** molecules, found on all nucleated cells<sup>49</sup>. CD8<sup>+</sup> T cells are cytotoxic and can kill virus-infected cells. Multiple genes expressed only in CD8<sup>+</sup> T



cells, including CCL3, ANAX1, TIMD4 and MAGT1, were upregulated in the liver by filovirus infection (**Fig. 5, S6C**), indicating that bats mount a T cell response against the infection.

### **EBOV and MARV infection affects the vascular system**

The vascular system carries nutrients, oxygen and the cells and molecules involved in the immune response and inflammation. The proper functioning of the system requires control of iron metabolism, blood pressure, and blood coagulation. We found that expression of genes involved in all these processes was affected by MARV and EBOV.

**Genes involved in iron homeostasis.** The absorption and availability of iron, an essential component of heme needed for oxygen transport, is tightly regulated<sup>50</sup>. Most iron is in hemoglobin (66%), the remainder is stored mostly in macrophages in the liver, which take up iron through the CD163 receptor. Iron is exported from macrophages and absorbed from food<sup>51</sup> through ferroportin (SLC40A1/FPN1).

MARV and EBOV changed the expression of multiple genes involved in iron homeostasis. Hepcidin (HAMP)<sup>52</sup>, which controls iron homeostasis by binding ferroportin, leading to its degradation as well as blocking the export of iron, was induced in infected livers (**Fig. 5, S8 Table 1**). Infection induced ceruloplasmin (an APP, **Table 1**), which enables the formation of the transferrin-iron complex and is also involved in processing copper<sup>53</sup>. In the cytosol, iron is bound to ferritin (comprised of a heavy chain, FTH1 and a light chain FTL), synthesized by cells in response to increased iron<sup>54</sup>. In mitochondria, iron is bound to FTMT, the mitochondrial ferritin<sup>55</sup>. Both FTH1 and FTMT were downregulated in MARV-infected bats but upregulated in EBOV-infected animals (**Fig. 5, S8**). MARV infection was associated with lowered hemoglobin expression, suggesting impairment of red blood cell production, potentially resulting in anemia. Consistent with this conclusion, CD164, which suppresses hematopoietic cell proliferation, was also upregulated by MARV infection (**Fig. 5, S8**), while HBB was suppressed EBOV-infected samples.

These observations suggest that hematopoiesis was impaired in MARV-infected bats, but not in EBOV-infected bats, and that regulation of iron by HAMP in bats might diverge from the homologous process in humans.

**Genes regulating vasodilation.** The primary means of blood pressure regulation is renal expression of renin, which converts angiotensinogen (AGT) to angiotensin I. Angiotensin converting enzyme (ACE) converts angiotensin I to angiotensin II, which constricts blood vessels to increase blood pressure. AGT is down regulated by MARV and EBOV infection, which would be expected to deplete the substrate for ACE, limiting the potential for blood pressure to increase even with upregulation of ACE (**Fig. 5, S8**). Low blood pressure would be consistent with our finding that filovirus infection induced expression of Prostaglandin I2 synthase (PTGIS), a potent vasodilator and inhibitor of platelet aggregation. However, blood pressure was not directly measured in the bats before euthanasia.

**Genes involved in blood coagulation.** Mechanisms that control blood pressure also impact coagulation. MARV and EBOV induced PTGIS, which reduces blood pressure and also inhibits platelet aggregation (**Fig. 5, S9**) and repressed AGT, the precursor of angiotensin II which enhances production of active plasmin to increase coagulation<sup>56</sup>. MARV and EBOV also induced CYP11B1, which increases cortisol that acts to reduce inflammation, and CYP11B2, which increases aldosterone levels that increases blood volume<sup>57</sup>. Together, these would be expected to reduce the effects of inflammation on the vascular system.

## **DISCUSSION**

Recently, multiple high-impact pathogens associated with bats have emerged or re-emerged, such as EBOV, MERS-CoV and SARS-CoV-2. As a result, the role of bats as reservoirs for a diverse array of viruses and their ability to tolerate viral infections that cause severe disease in humans has become a topic of considerable interest. A number of hypothesis have been proposed to explain this unique aspect of bat biology. Most are centered on the innate immune system. In these hypotheses, various aspects of bat innate immunity are either more or less potent than their human counterparts. One hypothesis in posits that some bat species<sup>22–24</sup> constitutively express interferons, leading to a basal level of innate immune activation. Overall, prior work with filoviruses demonstrating that the innate response in bat cells is robust, and similar to that observed in human cell lines<sup>26</sup> is inconsistent with this hypothesis. Another hypothesis suggests that components of the innate immune response (e.g., STING/TMEM173) are less effective in bats<sup>25</sup>, allowing viruses to survive in the host. Although this mechanism helps to explain the ability of bats to serve as reservoirs for a diverse range of viruses, it is less useful in explaining the ability of bats to survive and clear infection and may indicate at the involvement of the adaptive immune system in virus clearance.

All MARV-inoculated bats were productively infected, and our virology and histopathology data in MARV-infected bats are consistent with previous reports, including viral replication in the mammary glands and testes<sup>13</sup>. Evidence of successful, if limited, infection was identified in two of three EBOV inoculated animals. In particular, virus was detected by plaque assay in the livers of two of three animals, and immunohistochemistry identified a small number of foci in the liver of one animal. This contrasts with prior reports<sup>58</sup> and suggests that ERBs may not be truly refractory to EBOV infection. However, given the very low titers detected, and the limited nature of the observed immunostaining, it is unlikely that the virus could be maintained in animals in nature.

Our transcriptome analysis shows that the majority of interferon response genes are not divergent from their human homologs, consistent with prior observations that the innate responses are quite similar between human and bat cell lines<sup>26</sup>. This implies that other systems are involved.

We developed a framework to understand the observations with the interconnections between various systems as pertains to our study shown in Fig. 6. A key feature of filovirus infection is an inflammatory response leading to the expression of APPs and stimulation of M1 macrophages. C-reactive protein (CRP), which binds to micro-organisms, assists in complement binding to foreign and damaged cells, and enhances phagocytosis by macrophages (opsonin-mediated phagocytosis)<sup>59</sup> appears to be absent in bats, based on the lack of CRP sequences in our mRNA-seq data. In mice, CRP is not an acute phase protein<sup>60</sup>, and as such, it is unclear if this apparent lack of CRP is consequential in regards to the innate immunity of bats. Aside from CRP, however, the other APPs are conserved. We found evidence that the effector component of the antibody response may be weakened by incomplete complement activation. This is consistent with the previous reports that antibody-mediated virus neutralization is not the dominant mechanism of filovirus clearance in *R. aegyptiacus* bats<sup>61</sup>. The robust CD8+ T cell activity implied by our mRNA-seq data suggests that control and clearance of filovirus infection in bats may instead depend upon a robust T cell response. This is consistent with what is known in humans, where individuals who recover from filovirus infections tend to mount robust T cell responses<sup>62–64</sup>, and have higher levels of CD40L expression, a marker for T cell activity<sup>64</sup>.

The macrophage response was one of the more notable points of divergence between the human response to filovirus infection and what we observed in infected bats. We identified markers of both M1 and M2

macrophages in ERBs infected with MARV, suggesting that macrophage populations in the animals were in the process of switching from the classically pro-inflammatory M1 polarization to the M2 state, which is conventionally associated with anti-inflammatory processes, tissue repair, and regeneration. In particular, the modulation of the innate response facilitated by M2 macrophages is important for T cell mediated clearing of the virus. In EBOV-infected animals, where viral replication was far more limited, our sequencing data indicate that the macrophage population was further along in the transition to M2 polarization by the time of euthanasia. The generalized anti-inflammatory state observed in bats during filovirus infection, especially the early switch to M2 macrophage polarization, may be key to preventing the immunopathology associated with filovirus infection in humans, including cytokine storm and DIC. Supporting this, an mRNA-seq study conducted with PBMCs isolated from EBOV-infected humans found that individuals who succumbed to disease showed stronger upregulation of interferon signaling and acute phase response-related genes than survivors during the acute phase of infection<sup>65</sup>, suggesting that a tempered response may be more beneficial.

Our data suggest that the vascular response in bats differs from that in humans. Humans infected with EBOV or MARV frequently present with hemorrhagic manifestations and dysregulated coagulation in the form of disseminated intravascular coagulation<sup>66</sup>. We identified transcriptional patterns consistent with vasodilation and reduced potential for coagulation. This could result in a state in which blood pressure is lower than normal, and coagulation is reduced. This state may be protective, as it might be expected to prevent DIC. Our findings are consistent with results from a study in humans infected with EBOV<sup>67</sup> which analyzed 55 biomarkers in blood. This report found that viremia was associated with elevated levels of tissue factor and tissue plasminogen activator, consistent with coagulopathy.

Our results suggest that reducing the hyperinflammatory response<sup>68</sup> or controlling the coagulopathies<sup>69</sup> in humans during filovirus infection may have a therapeutic benefit by preventing damage to the host and allowing other processes to clear the infection. This could be achieved by the inhibition of IL-6 by agents such as siltuximab (Sylvant)<sup>70</sup>, or by targeting the IL-6 receptor via an antibody such as tocilizumab (Actemra)<sup>71</sup>

In bats, filovirus infection upregulates MGST1 and MGST2 which both induce leukotrienes (LTC<sub>4</sub>) and prostaglandin E, both of which are mediators of inflammation<sup>33</sup>. This is a potential druggable target, as these are targeted by several therapeutic agents. Thus, this inflammation could also be targeted by another class of anti-inflammatory agents such as LTC<sub>4</sub> inhibitors, used to treat asthma.

Our results also suggest that upon filovirus infection bats may naturally vasodilate and reduce their blood pressure (mimicking the action of ACE inhibitors) while the endothelial system becomes anti-thrombotic. Field trials of ACE inhibitors and statins in human Ebola virus disease have already seen some success<sup>72</sup>. Along these lines, another potentially useful drug is prostaglandin I<sub>2</sub> (PGI<sub>2</sub>, known as epoprostenol as a drug), a powerful vasodilator and anti-coagulant that acts by binding to the prostacyclin receptor. This has potential for use in human filovirus infections as a means of emulating the physiological conditions (low blood pressure and coagulation) in bats that our data suggest may have protective effects<sup>73</sup>.

In humans, high levels of HAMP causes iron to be sequestered in the liver, reducing levels of iron in blood (lower ferritin). Our observations indicate that in EBOV infected bats high HAMP expression is decoupled from the levels of iron, as both ferritin and HAMP are induced. Thus, HAMP inhibitors, which are used to treat anemia, might recreate in humans the state seen in bats under filoviral infection. Two HAMP inhibitors,



Heparin<sup>74</sup> and erythropoietin (EPO)<sup>75,76</sup>, have additional beneficial effects, anti-coagulation and RBC synthesis respectively, which might make them particularly efficacious. Vitamin D is also a HAMP inhibitor<sup>77</sup>.

Broadly, the changes in gene expression patterns that we have observed in infected bats suggest that the pathways regulating coagulation, vasodilation, iron homeostasis, inflammation, the interferon response and the adaptive response contribute to the unique response of these animals to filovirus infection. The most important outcome of this systemic response appears to be a tempering of the overall response to infection, avoiding immunopathology. In particular, the anti-inflammatory state observed, and the altered state of the vascular system appear to be important to preventing pathology and facilitating the ultimate clearance of the virus.

## CONCLUSIONS

Our observations and analyses provide an experimental and computational framework for understanding the resistance of bats to filovirus infection. This framework has the potential to aid in the development of new strategies to effectively mitigate and treat the effects of filovirus infections in humans.

## Data

All data underlying the balloon plots is available as csv files on the filobat website (<http://katahdin.girihlet.com/shiny/bat/>). Additionally, a fasta file containing all the mRNA sequences used in our analysis is also available on the website. The raw sequencing reads will be deposited with GEO, and the filobat site has several tools for analysis and exploration of data.

## MATERIALS AND METHODS

### Experimental methods

**Viruses.** Recombinant wild-type EBOV, strain Mayinga, was recovered from the full-length clone and support plasmids in HEK 293T cells and passaged twice in Vero E6 cells for amplification<sup>29</sup>. Recombinant wild-type MARV, strain Uganda, was recovered similarly in BHK-21 cells<sup>78</sup> and passaged twice in Vero E6 cells for amplification.

**Bat experimental protocol.** All animal procedures were performed in compliance with protocols approved by the Institutional Animal Care and Use Committee at the University of Texas Medical Branch at Galveston.

Adult ERBs were obtained from a commercial source and quarantined for 30 days under ABSL-2 conditions. Animals were implanted with microchip transponders for animal ID and temperature data collection. For studies with EBOV and MARV, animals were transferred to the Galveston National Laboratory ABSL-4 facility. Animals were segregated into groups of three. Except for one MARV-infected male, all bats were female. Each group was housed in a separate cage for inoculation with the same virus. After acclimation to the facility, animals were anesthetized with isoflurane and infected subcutaneously in the scapular region with  $10^5$  focus forming units (FFU; titrated on Vero E6 cells) of EBOV or MARV. Every other day, animals were anesthetized by isoflurane, weighed, temperature was determined via transponder, and 100-150  $\mu$ L of blood was collected from the propatagial vein. Blood was inactivated in 1 mL of TRIzol reagent (Thermo-Fisher Scientific). Samples were then removed from ABSL-4 containment, and RNA was extracted. Droplet-digital RT-PCR (ddRT-PCR) with primers specific to the nucleoprotein (NP) gene was used to detect viremia. If fewer than  $10^6$  MARV RNA copies/mL viremia were detected in a MARV-inoculated bat, the animal was observed for additional 2 days to allow the animal to reach a higher viral RNA load. All EBOV-inoculated bats were

euthanized 48 hours after the first detection of viremia, regardless of viral RNA load. Animals were euthanized under deep isoflurane sedation via cardiac exsanguination confirmed by bilateral open chest. Tissues were collected (listed in **Table S1**) and immediately homogenized in an appropriate volume of TRIzol reagent and stored at -80°C. 1 cubic centimeter (cc) tissue sections were homogenized in minimal essential media (MEM) supplemented with 10% fetal bovine serum and stored at -80°C. Additional tissue sections were fixed in 10% neutral buffered formalin for histopathology. Tissues and PBMCs were also collected from three uninfected control animals.

**Leukocyte isolation.** Leukocytes were isolated using ACK lysis buffer (Gibco). Ten volumes of lysis buffer were added to whole blood, incubated for 2-3 minutes, and then neutralized with complete DMEM media containing 10% FBS. Following neutralization, samples were centrifuged at 250 g for 5 minutes at 4°C, after which the supernatant was decanted from the pellet. This process was repeated several times per sample until a white pellet of cells free of contaminating red blood cells remained. Because density gradient purification was not performed on these samples prior to or after red blood cell lysis, these leukocyte preparations were assumed to contain granulocytes in addition to PBMCs.

**mRNA sequencing.** Total RNA was isolated from bat tissues using Ambion's RNA isolation and purification kit. For most samples, polyA-tailed mRNA was selected using beads with oligo-deoxythymidine and then fragmented. A few samples with poor RIN (RNA Integrity Number) scores were treated with Ribominus (targeting human ribosomal RNA) to enrich for polyA-tailed mRNA before fragmentation. cDNA was synthesized using random hexamers and ligated with bar-coded adaptors compatible with Illumina's NextSeq 500 sequencer. A total of 88 samples were sequenced on the NextSeq 500, as 75 base pair single reads.

## Analytical methods

**Bat mRNA sequence database.** The extant bat genomes are nowhere near completion and a comprehensive mRNA database does not exist. Thus, for this study, we constructed a custom non-redundant reference bat mRNA sequence database, which is available at <https://katahdin.girihlet.com/shiny/bat/>. We started with existing genome annotations<sup>79</sup>. The complications arising from splice variants were avoided by keeping only the longest transcript for each gene. We added missing annotations/sequences (e.g., CYP11B2 and PLG) to our database by assembling reads from our own sequence data. These required custom scripts as there often was not enough reads covering a transcript, which precluded the use of standard assembly tools. The gene sequences were collected from different bat species, so error-free reads might not map perfectly to the transcripts in the database. The database has sequences of 18,443 bat mRNAs, and include EBOV and MARV sequences, the infectious agents used in our studies. The genes were identified by homology to mouse and human genes, 16,004 bat genes had high similarity to human or mouse homologues, as defined by BLASTn with default settings identifying matches spanning the length of the mRNA.

The set of remaining genes (2439) were labelled as divergent. Of these, 1,548 transcripts could be identified by increasing the sensitivity of BLASTn by reducing the word-size from 11 to 9, which is equivalent to matching at the protein level. Of the remaining 891 putative transcripts, homologues for 182 could be identified on the basis of partial homology and domain structure, while the remainder (709 sequences whose names start with UNDEF) belonged to one of four classes, 1) aligned to un-annotated transcripts in the human genome, 2) non-

coding RNAs, 3) transcripts unique to bats, or 4) assembly errors. We use capitalizations to represent bat gene symbols, as in the human gene nomenclature.

To identify genes within these divergent set that are relevant to our study, we then selected a subset of genes that had good expression (defined as  $\text{tpm} > 20$ ) in at least one class of liver samples (MARV-, EBOV- or mock-infected) and responsive in either MARV- or EBOV- infected bat livers, which we defined as up- ( $\log_2$  ratio  $> 0.6$ ), or down- ( $\log_2$  ratio  $< -0.6$ ) regulated. We were left with 151 genes that are the foundation of our analyses of pathways involved in the response to filoviruses (**Tables S3-S8**).

**Expression Analyses.** To determine transcript expression levels, we used Kallisto, because this tool uses pseudo-alignments and is relatively more tolerant of errors/variants in reads<sup>80</sup>, which we expect here because the reads and mRNA sequences in the database do not always come from the same species. Kallisto uses a parameter “k” while indexing the database to specify how sensitive it is to matches with smaller k values leading to more spurious hits. We empirically determined  $k=23$  to be an appropriate parameter value with which to index the reference mRNA dataset. We used the transcripts-per-million (tpm) value as the transcript expression levels to determine changes in expression across samples.

We used viral transcripts to identify infected samples, which has previously helped us to identify and correct mistakes of annotation in some of the cell line data and also identified a problem with a published dataset<sup>81</sup>, where all the naïve (uninfected) samples showed signs of viral infection. Furthermore, to ensure there was no mislabeling of tissue samples from different bats, we used single nucleotide variants in the sequenced reads to confirm that all tissue samples from an individual had the same set of variants.

Using clustering based on expression profiles and considering individual interferon responsive genes, it was clear that one non-infected control bat liver sample (labeled *cb1* in the shiny tool) was reacting to some stimulus (injury or infection) compared to the other two control samples (*cb2* and *cb3* in the shiny tool); Since we are interested in the innate response to infections, we had to exclude *cb1* from the controls, but *cb1* data are available for exploration in the *filobat* tool.

As such, most of our analyses concentrated on liver RNA transcripts since it had the strongest response and the genes indicated that a variety of cell types were involved in the response, capturing the systemic nature of the response. Liver function impacts a wide range of systems involving inflammation, iron homeostasis, and blood pressure. Other organs, such as kidney and spleen provide additional support for what is observed in the liver. For some genes, we also used the transcriptional response in kidney (Renin) and/or spleen (STING) in order to understand the regulation of pathways (e.g., Renin is expressed in kidney and regulates the blood pressure system).

**Tools for data exploration and interrogation.** To allow exploration of the data across various samples on a gene-by-gene basis, as well as analysis of viral expression in the samples, we developed a browser-based tool, *filobat*, using *Shiny* in R (<http://katahdin.girihlet.com/shiny/bat/>). Samples can also be compared using scatter plots and hierarchical clustering.

**Statistics.** Large changes in expression profiles were readily detected by comparing averages across replicates, since such changes are less affected by noise; however, subtle changes (less than 2-fold) were difficult to reliably detect due to lack of power in the sample size and variability between samples and are mostly not considered.

**Pathway analyses.** A fundamental assumption underlying our study is that bats are mammals that possess innate and adaptive responses to infections that roughly mirror those seen in humans. The data from comparative filovirus infections in human and bat cell lines supports this assumption<sup>26</sup>. To identify pathways of interest from particular genes, we used GO/pathways annotations of the human counterparts<sup>82</sup> and grouped them into functions that provided themes in the dataset. Using these themes, we identified other differentially expressed genes sharing these themes, identified by the GO annotations for human and mouse genes. This allowed us to build a picture of the pathways triggered by filovirus infections and delineate the ways in which the systemic bat responses differs from those seen in humans.

## ACKNOWLEDGEMENTS

Oliver Fregoso provided many insightful comments, suggestions, and encouragement for our approach. Discussions with Yelena Ginzburg on the role of HAMP in iron homeostasis were extremely helpful. Radhika Patnala and Arne Fabritius of Sci-Illustrate made many of the figures. Yuri Lazebnik was immensely helpful, by editing and streamlining the text and gave many critical comments to clarify our message. Viviana Simon read early versions and gave suggestions and encouragement. RS acknowledges partial support from grant R01-AI136916 from NIH/NIAID. Primary funding for this work (CFB, AB, RS) was through the grant HDTRA1-16-1-0033 from the Defense Threat Reduction Agency.

## REFERENCES

1. Rougeron, V., Feldmann, H., Grard, G., Becker, S. & Leroy, E. M. Ebola and Marburg haemorrhagic fever. *J. Clin. Virol.* **64**, 111–119 (2015).
2. CDC, M. Outbreak Table | Marburg Hemorrhagic Fever | CDC. <https://www.cdc.gov/vhf/marburg/resources/outbreak-table.html>.
3. WHO. Ebola health update - DRC, 2019. <https://www.who.int/emergencies/diseases/ebola/drc-2019>.
4. Geisbert, T. W. *et al.* Pathogenesis of Ebola Hemorrhagic Fever in Primate Models. *Am J Pathol* **163**, 2371–2382 (2003).
5. Towner, J. S. *et al.* Isolation of genetically diverse Marburg viruses from Egyptian fruit bats. *PLoS Pathog* **5**, e1000536 (2009).
6. Amman, B. R. *et al.* Seasonal pulses of Marburg virus circulation in juvenile *Rousettus aegyptiacus* bats coincide with periods of increased risk of human infection. *PLoS Pathog.* **8**, e1002877 (2012).
7. Amman, B. R. *et al.* Isolation of Angola-like Marburg virus from Egyptian rousette bats from West Africa. *Nat Commun* **11**, 510 (2020).
8. Schuh, A. J. *et al.* Modelling filovirus maintenance in nature by experimental transmission of Marburg virus between Egyptian rousette bats. *Nat Commun* **8**, 14446 (2017).
9. Paweska, J. T. *et al.* Lack of Marburg Virus Transmission From Experimentally Infected to Susceptible In-Contact Egyptian Fruit Bats. *J. Infect. Dis.* **212 Suppl 2**, S109-118 (2015).
10. Jones, M. E. B. *et al.* Clinical, Histopathologic, and Immunohistochemical Characterization of Experimental Marburg Virus Infection in A Natural Reservoir Host, the Egyptian Rousette Bat (*Rousettus aegyptiacus*). *Viruses* **11**, (2019).
11. Paweska, J. T. *et al.* Virological and Serological Findings in *Rousettus aegyptiacus* Experimentally Inoculated with Vero Cells-Adapted Hogan Strain of Marburg Virus. *PLoS One* **7**, (2012).

12. Amman, B. R. *et al.* Oral shedding of Marburg virus in experimentally infected Egyptian fruit bats (*Rousettus aegyptiacus*). *J. Wildl. Dis.* **51**, 113–124 (2015).
13. Jones, M. E. B. *et al.* Experimental Inoculation of Egyptian Rousette Bats (*Rousettus aegyptiacus*) with Viruses of the Ebolavirus and Marburgvirus Genera. *Viruses* **7**, 3420–3442 (2015).
14. Schuh, A. J. *et al.* Egyptian rousette bats maintain long-term protective immunity against Marburg virus infection despite diminished antibody levels. *Sci Rep* **7**, 8763 (2017).
15. Leroy, E. M. *et al.* Human Ebola outbreak resulting from direct exposure to fruit bats in Luebo, Democratic Republic of Congo, 2007. *Vector Borne Zoonotic Dis.* **9**, 723–728 (2009).
16. Mari Saéz, A. *et al.* Investigating the zoonotic origin of the West African Ebola epidemic. *EMBO Mol Med* **7**, 17–23 (2015).
17. Schuh, A. J., Amman, B. R. & Towner, J. S. Filoviruses and bats. *Microbiol. Aust.* **38**, 12–16 (2017).
18. Yuan, J. *et al.* Serological evidence of ebolavirus infection in bats, China. *Viol. J.* **9**, 236 (2012).
19. Olival, K. J. *et al.* Ebola virus antibodies in fruit bats, bangladesh. *Emerging Infect. Dis.* **19**, 270–273 (2013).
20. Pourrut, X. *et al.* Large serological survey showing cocirculation of Ebola and Marburg viruses in Gabonese bat populations, and a high seroprevalence of both viruses in *Rousettus aegyptiacus*. *BMC Infect. Dis.* **9**, 159 (2009).
21. Krähling, V. *et al.* Establishment of fruit bat cells (*Rousettus aegyptiacus*) as a model system for the investigation of filoviral infection. *PLoS Negl Trop Dis* **4**, e802 (2010).
22. Zhou, P. *et al.* Contraction of the type I IFN locus and unusual constitutive expression of IFN- $\alpha$  in bats. *Proc. Natl. Acad. Sci. U.S.A.* **113**, 2696–2701 (2016).
23. Glennon, N. B., Jabado, O., Lo, M. K. & Shaw, M. L. Transcriptome Profiling of the Virus-Induced Innate Immune Response in *Pteropus vampyrus* and Its Attenuation by Nipah Virus Interferon Antagonist Functions. *J. Virol.* **89**, 7550–7566 (2015).
24. Pavlovich, S. S. *et al.* The Egyptian Rousette Genome Reveals Unexpected Features of Bat Antiviral Immunity. *Cell* **173**, 1098–1110.e18 (2018).
25. Xie, J. *et al.* Dampened STING-Dependent Interferon Activation in Bats. *Cell Host Microbe* **23**, 297–301.e4 (2018).
26. Kuzmin, I. V. *et al.* Innate Immune Responses of Bat and Human Cells to Filoviruses: Commonalities and Distinctions. *J. Virol.* **91**, (2017).
27. Becker, S., Spiess, M. & Klenk, H. D. The asialoglycoprotein receptor is a potential liver-specific receptor for Marburg virus. *J. Gen. Virol.* **76** ( Pt 2), 393–399 (1995).
28. Kushner, I. Acute phase reactants. *UpToDate* <https://www.uptodate.com/contents/acute-phase-reactants>.
29. Kushner, I. The phenomenon of the acute phase response. *Ann. N. Y. Acad. Sci.* **389**, 39–48 (1982).
30. Gabay, C. & Kushner, I. Acute-phase proteins and other systemic responses to inflammation. *N. Engl. J. Med.* **340**, 448–454 (1999).
31. Gauldie, J., Richards, C., Harnish, D., Lansdorp, P. & Baumann, H. Interferon beta 2/B-cell stimulatory factor type 2 shares identity with monocyte-derived hepatocyte-stimulating factor and regulates the major acute phase protein response in liver cells. *Proc. Natl. Acad. Sci. U.S.A.* **84**, 7251–7255 (1987).
32. Moshage, H. J., Janssen, J. A., Franssen, J. H., Hafkenscheid, J. C. & Yap, S. H. Study of the molecular mechanism of decreased liver synthesis of albumin in inflammation. *J. Clin. Invest.* **79**, 1635–1641 (1987).



33. Dvash, E., Har-Tal, M., Barak, S., Meir, O. & Rubinstein, M. Leukotriene C 4 is the major trigger of stress-induced oxidative DNA damage. *Nat Commun* **6**, 1–15 (2015).
34. Wang, T. *et al.* HIF1 $\alpha$ -Induced Glycolysis Metabolism Is Essential to the Activation of Inflammatory Macrophages. *Mediators Inflamm.* **2017**, 9029327 (2017).
35. Mills, E. L. & O'Neill, L. A. Reprogramming mitochondrial metabolism in macrophages as an anti-inflammatory signal. *Eur. J. Immunol.* **46**, 13–21 (2016).
36. Krawczyk, C. M. *et al.* Toll-like receptor-induced changes in glycolytic metabolism regulate dendritic cell activation. *Blood* **115**, 4742–4749 (2010).
37. Tannahill, G. M. *et al.* Succinate is an inflammatory signal that induces IL-1 $\beta$  through HIF-1 $\alpha$ . *Nature* **496**, 238–242 (2013).
38. Nizet, V. & Johnson, R. S. Interdependence of hypoxic and innate immune responses. *Nat. Rev. Immunol.* **9**, 609–617 (2009).
39. Tan, Z. *et al.* Pyruvate dehydrogenase kinase 1 participates in macrophage polarization via regulating glucose metabolism. *J. Immunol.* **194**, 6082–6089 (2015).
40. Ferrante, C. J. *et al.* The adenosine-dependent angiogenic switch of macrophages to an M2-like phenotype is independent of interleukin-4 receptor alpha (IL-4R $\alpha$ ) signaling. *Inflammation* **36**, 921–931 (2013).
41. Imamura, R. & Matsumoto, K. Hepatocyte growth factor in physiology and infectious diseases. *Cytokine* **98**, 97–106 (2017).
42. Atri, C., Guerfali, F. Z. & Laouini, D. Role of Human Macrophage Polarization in Inflammation during Infectious Diseases. *Int J Mol Sci* **19**, (2018).
43. Parisi, L. *et al.* Macrophage Polarization in Chronic Inflammatory Diseases: Killers or Builders? *J Immunol Res* **2018**, (2018).
44. Helming, L. Inflammation: Cell Recruitment versus Local Proliferation. *Current Biology* **21**, R548–R550 (2011).
45. Jenkins, S. J. *et al.* Local macrophage proliferation, rather than recruitment from the blood, is a signature of TH2 inflammation. *Science* **332**, 1284–1288 (2011).
46. Murphy, M. P. Rerouting metabolism to activate macrophages. *Nat Immunol* 1–3 (2019) doi:10.1038/s41590-019-0455-5.
47. Agoro, R., Taleb, M., Quesniaux, V. F. J. & Mura, C. Cell iron status influences macrophage polarization. *PLOS ONE* **13**, e0196921 (2018).
48. Noris, M. & Remuzzi, G. Overview of Complement Activation and Regulation. *Semin Nephrol* **33**, 479–492 (2013).
49. Germain, R. N. T-cell development and the CD4–CD8 lineage decision. *Nat Rev Immunol* **2**, 309–322 (2002).
50. Knutson, M. D. Iron transport proteins: Gateways of cellular and systemic iron homeostasis. *J. Biol. Chem.* **292**, 12735–12743 (2017).
51. Prentice, A. M. *et al.* Hepcidin is the major predictor of erythrocyte iron incorporation in anemic African children. *Blood* **119**, 1922–1928 (2012).
52. Przybyszewska, J. & Żekanowska, E. The role of hepcidin, ferroportin, HCP1, and DMT1 protein in iron absorption in the human digestive tract. *Prz Gastroenterol* **9**, 208–213 (2014).

53. Wessling-Resnick, M. Crossing the Iron Gate: Why and How Transferrin Receptors Mediate Viral Entry. *Annu. Rev. Nutr.* **38**, 431–458 (2018).
54. Kohgo, Y., Ikuta, K., Ohtake, T., Torimoto, Y. & Kato, J. Body iron metabolism and pathophysiology of iron overload. *Int J Hematol* **88**, 7–15 (2008).
55. Gao, G. & Chang, Y.-Z. Mitochondrial ferritin in the regulation of brain iron homeostasis and neurodegenerative diseases. *Front Pharmacol* **5**, (2014).
56. Brown, N. J. & Vaughan, D. E. Role of Angiotensin II in Coagulation and Fibrinolysis. *Heart Fail Rev* **3**, 193–198 (1999).
57. Conway, E. M. Complement-coagulation connections. *Blood Coagulation & Fibrinolysis* **29**, 243 (2018).
58. Paweska, J. T. *et al.* Experimental Inoculation of Egyptian Fruit Bats (*Rousettus aegyptiacus*) with Ebola Virus. *Viruses* **8**, (2016).
59. Wu, Y., Potempa, L. A., El Kebir, D. & Filep, J. G. C-reactive protein and inflammation: conformational changes affect function. *Biol. Chem.* **396**, 1181–1197 (2015).
60. Du Clos, T. W. C-reactive protein as a regulator of autoimmunity and inflammation. *Arthritis Rheum.* **48**, 1475–1477 (2003).
61. Schuh, A. J. *et al.* Antibody-Mediated Virus Neutralization Is Not a Universal Mechanism of Marburg, Ebola, or Sosuga Virus Clearance in Egyptian Rousette Bats. *J. Infect. Dis.* **219**, 1716–1721 (2019).
62. McElroy, A. K. *et al.* Human Ebola virus infection results in substantial immune activation. *Proc. Natl. Acad. Sci. U.S.A.* **112**, 4719–4724 (2015).
63. Dahlke, C. *et al.* Comprehensive Characterization of Cellular Immune Responses Following Ebola Virus Infection. *J. Infect. Dis.* **215**, 287–292 (2017).
64. Reynard, S. *et al.* Immune parameters and outcomes during Ebola virus disease. *JCI Insight* **4**, (2019).
65. Liu, X. *et al.* Transcriptomic signatures differentiate survival from fatal outcomes in humans infected with Ebola virus. *Genome Biology* **18**, 4 (2017).
66. Feldmann, H. & Klenk, H.-D. Filoviruses. in *Medical Microbiology* (ed. Baron, S.) (University of Texas Medical Branch at Galveston, 1996).
67. McElroy, A. K. *et al.* Ebola hemorrhagic Fever: novel biomarker correlates of clinical outcome. *J. Infect. Dis.* **210**, 558–566 (2014).
68. Younan, P., Ramanathan, P., Graber, J., Gusovsky, F. & Bukreyev, A. The Toll-Like Receptor 4 Antagonist Eritoran Protects Mice from Lethal Filovirus Challenge. *MBio* **8**, (2017).
69. Rasmussen, A. L. *et al.* Host genetic diversity enables Ebola hemorrhagic fever pathogenesis and resistance. *Science* **346**, 987–991 (2014).
70. Schoels, M. M. *et al.* Blocking the effects of interleukin-6 in rheumatoid arthritis and other inflammatory rheumatic diseases: systematic literature review and meta-analysis informing a consensus statement. *Ann Rheum Dis* **72**, 583–589 (2013).
71. Jones, S. A., Scheller, J. & Rose-John, S. Therapeutic strategies for the clinical blockade of IL-6/gp130 signaling. *J Clin Invest* **121**, 3375–3383 (2011).
72. Fedson, D. S. & Rordam, O. M. Treating Ebola patients: a ‘bottom up’ approach using generic statins and angiotensin receptor blockers. *International Journal of Infectious Diseases* **36**, 80–84 (2015).
73. Cacione, D. G., Macedo, C. R. & Baptista-Silva, J. C. Pharmacological treatment for Buerger’s disease. *Cochrane Database of Systematic Reviews* (2016) doi:10.1002/14651858.CD011033.pub3.

74. Poli, M. *et al.* Heparin: a potent inhibitor of hepcidin expression in vitro and in vivo. *Blood* **117**, 997–1004 (2011).
75. Arezes, J. *et al.* Erythroferrone inhibits the induction of hepcidin by BMP6. *Blood* **132**, 1473–1477 (2018).
76. Nai, A. *et al.* Limiting hepatic Bmp-Smad signaling by matriptase-2 is required for erythropoietin-mediated hepcidin suppression in mice. *Blood* **127**, 2327–2336 (2016).
77. Bacchetta, J. *et al.* Suppression of Iron-Regulatory Hepcidin by Vitamin D. *J Am Soc Nephrol* **25**, 564–572 (2014).
78. Albariño, C. G. *et al.* Development of a reverse genetics system to generate recombinant Marburg virus derived from a bat isolate. *Virology* **446**, 230–237 (2013).
79. Jebb, D. *et al.* Six new reference-quality bat genomes illuminate the molecular basis and evolution of bat adaptations. *bioRxiv* 836874 (2019) doi:10.1101/836874.
80. Bray, N. L., Pimentel, H., Melsted, P. & Pachter, L. Near-optimal probabilistic RNA-seq quantification. *Nature Biotechnology* **34**, 525–527 (2016).
81. Hölzer, M. *et al.* Differential transcriptional responses to Ebola and Marburg virus infection in bat and human cells. *Scientific Reports* **6**, 34589 (2016).
82. The Gene Ontology Resource: 20 years and still GOing strong. *Nucleic Acids Res* **47**, D330–D338 (2019).

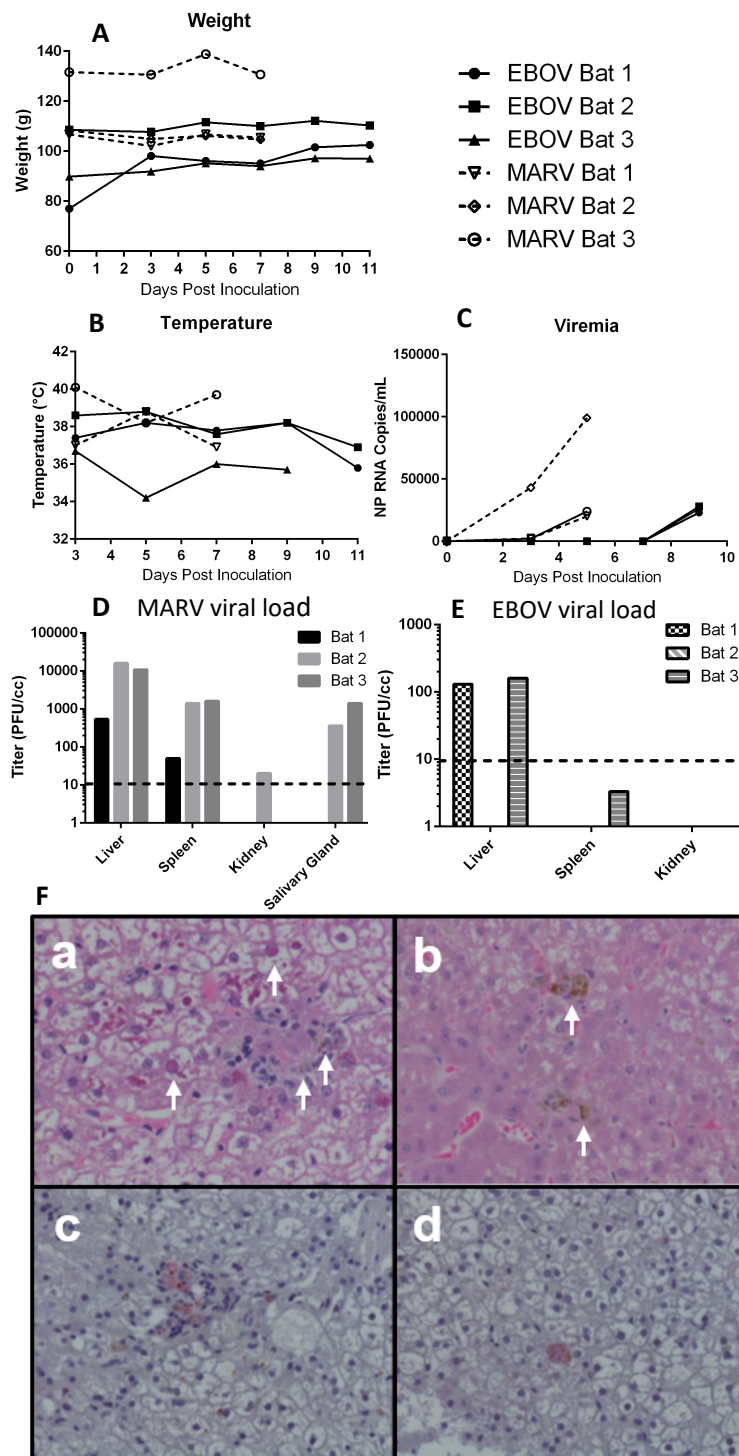


**Figure 1: Bat infection with filovirus, MARV and EBOV. Time course after infection for A) Weight, B) temperature and C) viremia (MARV Bat 2 sensor failed). Viremia measured in total RNA extracted from whole blood via ddRT-PCR targeting the viral NP gene. Animals were euthanized 48 hours after last viremic timepoint. Tissue viral loads (D and E) were determined by conventional plaque assay on Vero E6 cells. F) Histopathology in EBOV infected livers showing F.a) EBOV Bat 1 liver with marked histopathological changes, including cytoplasmic and nuclear inclusions (arrows), F. b.) EBOV Bat 2 liver displaying a less dramatic presentation compared to Bat 1, F.c) IHC detection of filovirus antigen in EBOV Bat 1 liver, and F.d.) IHC detection of EBOV VP40 in EBOV Bat 1 liver.**

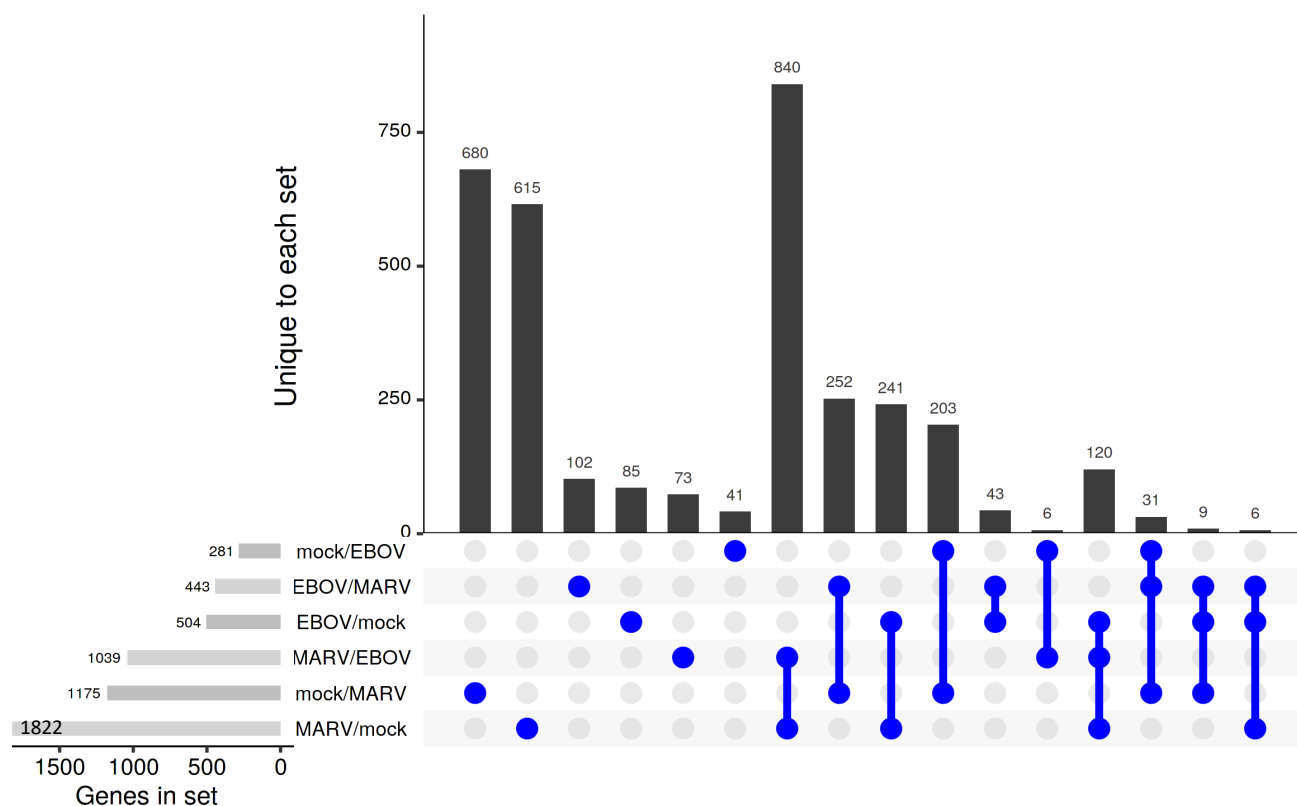


**Figure 2: Upset plot for data from bat liver.** Upset plots are an alternative to complex Venn diagrams. In the plot, *mock* refers to mock-infected bats, *EBOV* to EBOV-infected bats, and *MARV* to MARV-infected bat livers. Each row in the lower panel represents a set, with the corresponding colored bars at the lower left representing membership in the sets. There are six sets of genes, *EBOV/mock* comprises of genes at least 2-fold up regulated in EBOV infection, compared to the mock samples, while *mock/EBOV* is genes at least 2-fold down regulated in EBOV samples compared to the mock samples. The vertical blue lines with bulbs represent set intersections, the main bar plot (top) is number of genes unique to that intersection, so the total belonging to a set, say *mock/EBOV*, is a sum of the numbers in all sets that have *mock/EBOV* as a member ( $41+203+6+31=281$ ). For example, the last bar with 6 members is the set of genes common to *EBOV/MARV*, *EBOV/mock* and *MARV/mock*. Many more genes respond to infection by MARV than by EBOV. The EBOV-specific (*EBOV/MARV*) and MARV-specific (*MARV/EBOV*) genes, are mostly due to the different stages of infections when the samples were collected, the EBOV is cleared, while MARV is in the process of being cleared. Some in these two sets are likely due to host responses specific to the viral VP40, VP35 and VP24 genes.



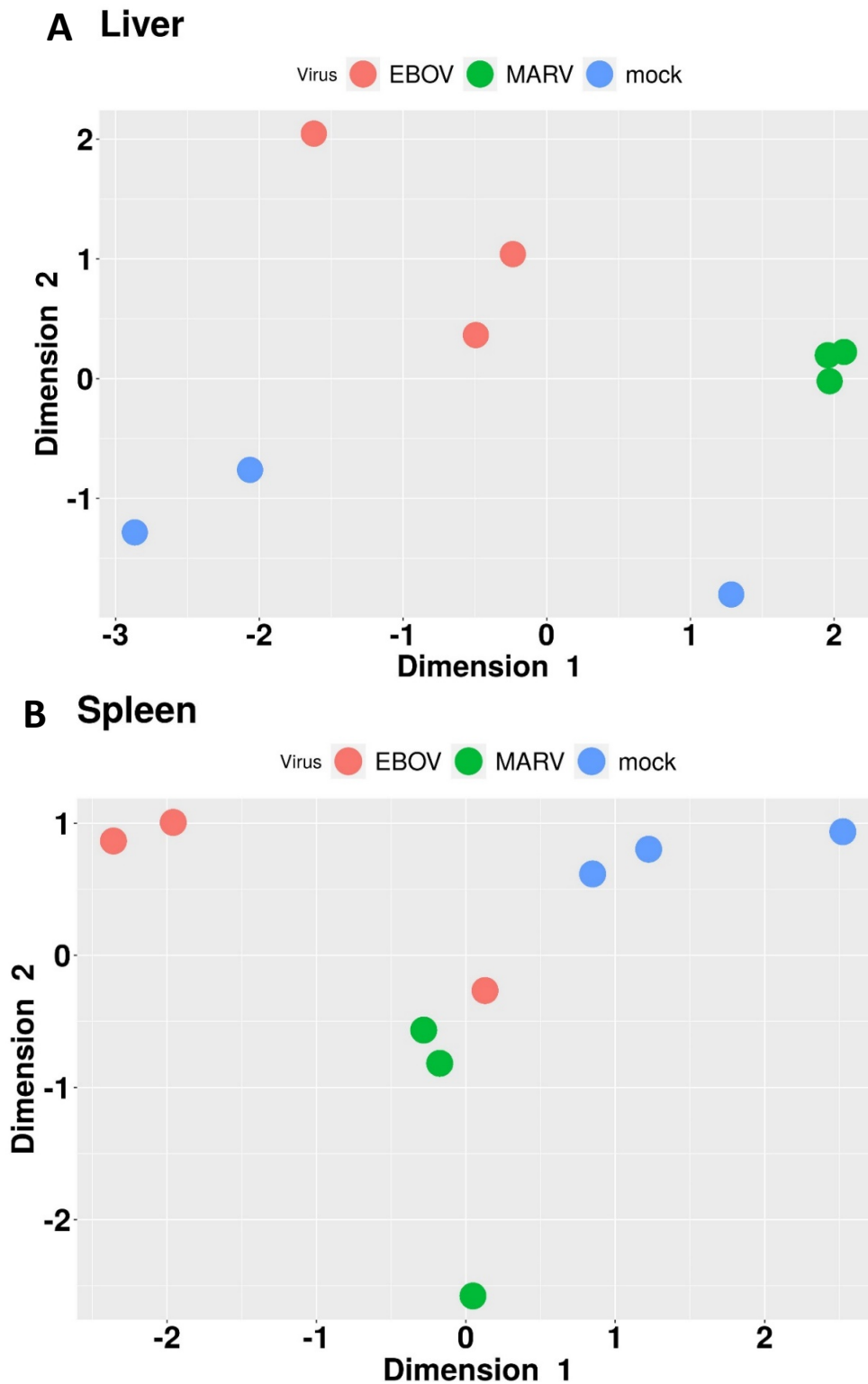


**Figure 3: MDS plots along the two leading dimensions (the x and y axis respectively).** There is clear separation between different infections (MARV and EBOV) and the mock-infected **A**) Liver and **B**) Spleen samples. Despite the paucity of viral transcripts, Spleen and other tissues (PBMC, kidney, salivary gland, lung, large and small intestine, **Fig. S1**) also exhibit virus-specific signatures, implying the response to filovirus infections extends to the whole bat. The top panel shows a mock-infected liver sample (the blue dot in lower right) that seems to be different from the other two mock-infected samples. This bat seems to be reacting to some stimulus, either an infection or injury, and has been excluded from our analysis.

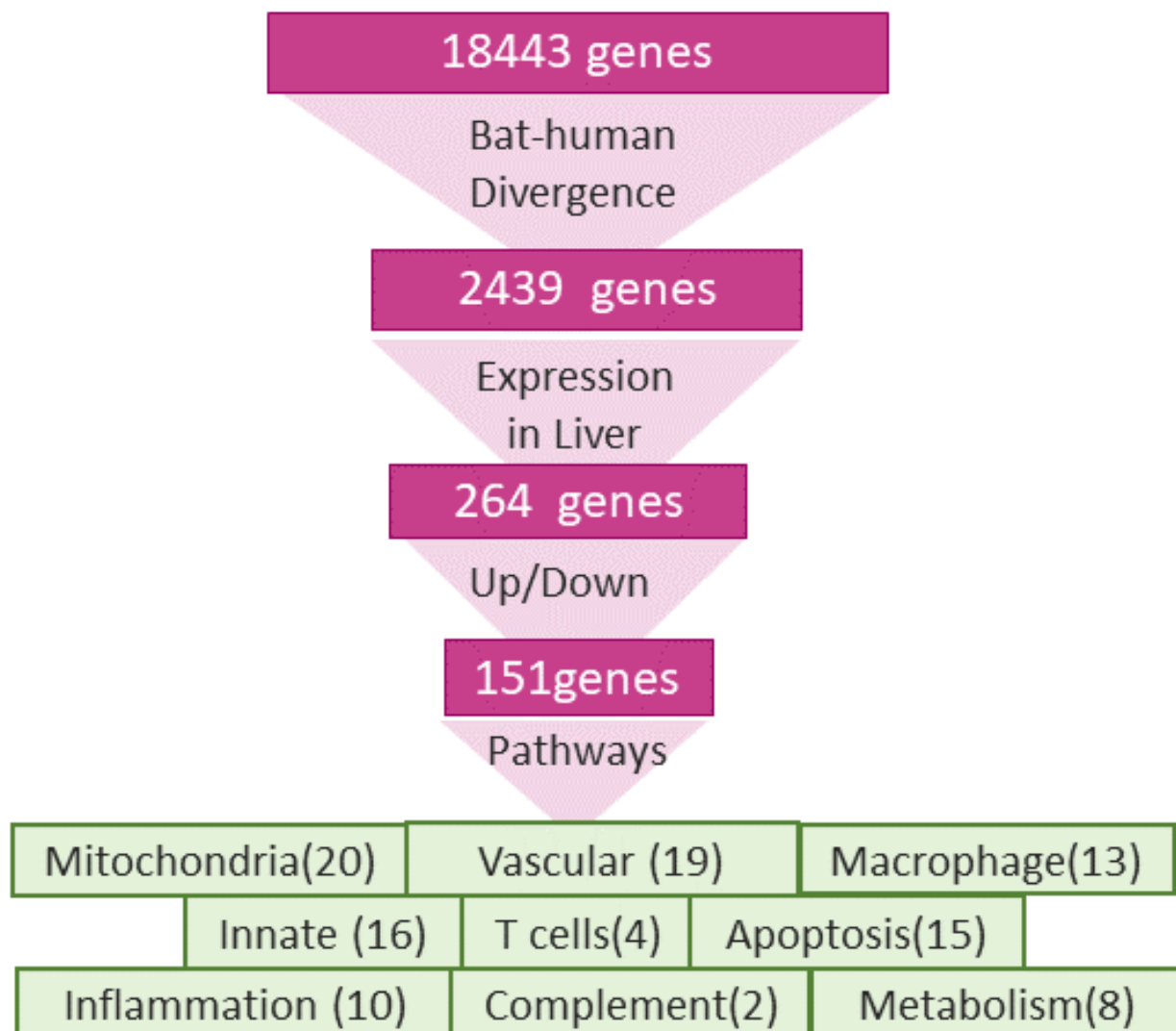


**Figure 4. Pathways from mRNA-seq.** The process used in the paper to identify pathways relevant to the bat's resilience in the face of filoviral infection. It is assumed that most homologous genes perform similar functions in bats and humans. Bat genes evolutionarily divergent from their human homologs have a greater probability of having altered functions. Of these, those responsive in liver to filovirus infection were identified. The pathways they influence were explored to evaluate the systemic response to filovirus infections in bats and identify key differences from human responses. The vascular system (Blood pressure, Coagulation and Iron homeostasis) was a prominent pathway. Glycolysis, which is controlled by Hypoxia, shifts the balance between M1 and M2 states of macrophage activation. These changes create an anti-inflammatory state that modulate the response and allows the adaptive immune system to clear the infection. The complement system is not fully activated, likely compromising the antibody response, but T cells are active and play a major role in clearing the infection. The pathways are interconnected, as shown in **Fig. 6**.

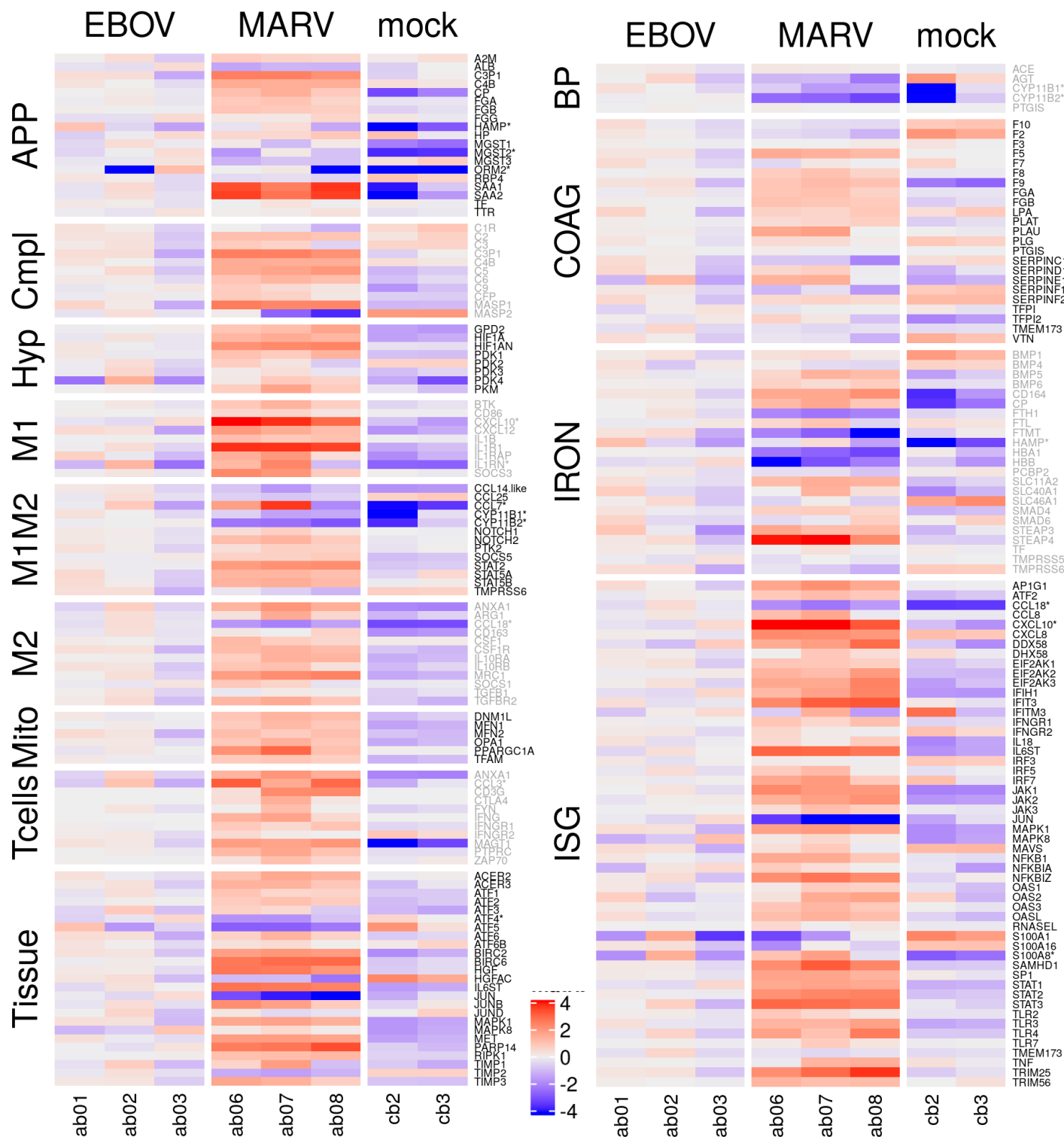


**Figure 5. Regulation of pathways by MARV and EBOV infections in liver.** On the left are genes in Acute Phase Response (APP), Complement (Cmpl), Hypoxia (Hyp), Tissue regeneration/apoptosis (Tissue), and genes specific to macrophages in the M1 state (M1), M2 state (M2) or both (M1M2). On the right are genes for Blood Pressure(BP), Coagulation (COAG), iron homeostasis (IRON) and Interferon stimulated genes (ISG). The columns show the three liver samples from EBOV-infected bats, and MARV-infected bats, as well as two un-infected samples. The values are log<sub>2</sub> of the fpm values, with the mean value of the EBOV samples subtracted out. Broadly, majority of the genes are in a quiescent, low expression state in the mock infected samples, and get stimulated upon infection, with large effects in the case of MARV and intermediate effects in the case of EBOV. A \* after a gene name signifies the bat version is diverged from its human counterpart. **Fig. S10A** and **S10B** show corresponding figures for kidney and spleen.

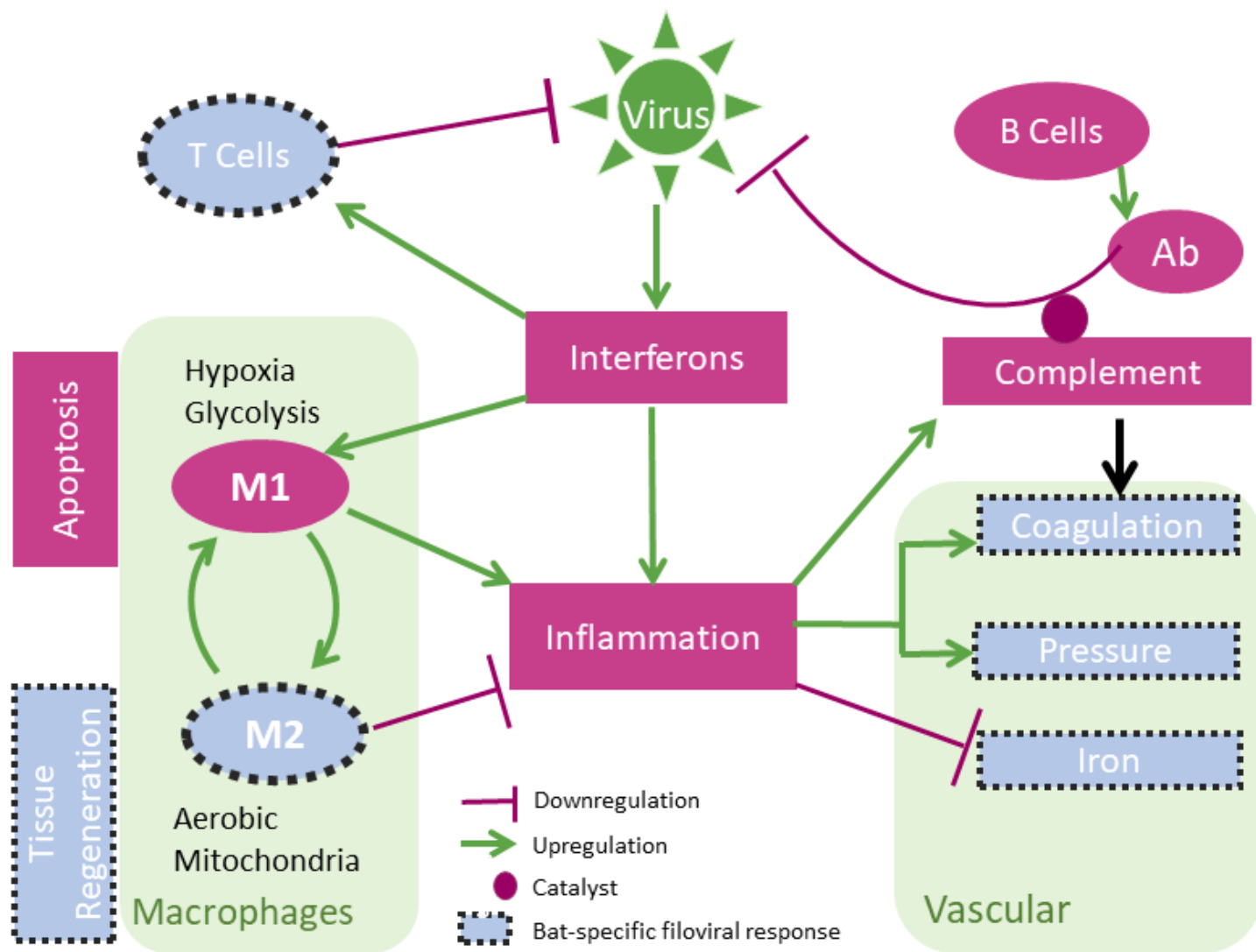


**Figure 6: Overview of the response to filovirus replication.** Interferon stimulated genes (ISG Fig. 5,S2,S3) cause inflammation, which triggers an acute phase response (APR, Table 1, Fig. 5), leading to a cascade of vascular events, affecting regulation of HAMP (iron, Fig. 5,S7), coagulation (Fig. 5,S9) blood pressure (Fig. 5,S8) and M1 macrophage stimulation (Fig. 5,S4,S5). The inflammatory M1 macrophages are stimulated by infection and phagocytize infected cells and promote apoptosis. Over the course of MARV or EBOV infection, they get converted to anti-inflammatory M2 macrophages. Fatty acid oxidation and mitochondrial activity are up, which are hallmarks of M2 macrophages (Fig 5,S4,S5,S6A). The complement system is incompletely stimulated by the acute phase response, leading to potentially restricted antibody activity (Fig. 5,S6B). Blood pressure (Fig. 5,S8) and coagulation (Fig. 5,S9) are down regulated in MARV and EBOV infection, while iron levels (Fig. 5,S7) are high, especially in EBOV infection (contrary to the levels of HAMP). T cell (CD8+) activity (Fig. S6C) is also upregulated, leading to the infection being cleared. Dotted boundaries show functions that likely distinguish the response of the bats from the human response to filovirus infections.

<b>Positive APPs</b>	<b>MARV (fold change)</b>	<b>EBOV (fold change)</b>	<b>Mock (tpm)</b>
Serum Amyloid A 1 (SAA1)	21X	3X	6858
Serum Amyloid A 2 (SAA2)	39X	5X	440
Ceruloplasmin (CP)	10X	5X	129
HAMP*	8.5X	10X	211
Orosomucoid 2 Alpha1-Acid glycoprotein (ORM2*)	34X	47X	14
Microsomal Glutathione S-Transferase MGST1	4X	4X	277
MGST2*	11X	16X	5.5
MGST3	0.4X	0.7X	461
Fibrinogen (FGA)	2X	1X	1277
Fibrinogen (FGB)	2X	1X	9007
Fibrinogen(FGG)	1X	1X	6070
C4B	2X	1X	1015
C3P1	6X	1X	31
Haptoglobin (HP)	1.1X	0.7X	15906
Alpha2-Macroglobulin (A2M)	1.3X	1X	409
C-reactive protein (CRP)	N/A	N/A	N/A
<b>Negative APPs</b>			
Albumin (ALB)	0.6X	1.2X	51400
Transferrin (TF)	1X	1X	22856
Transthyretin (TTR)	2X	2X	1
Retinol Binding protein (RBP4)	0.5X	0.6X	3107

**Table 1 Acute Phase Proteins in livers respond strongly to inflammatory cytokines (IL-6, TNF $\alpha$  etc.).** Inflammation usually upregulates positive APPs, while negative APPs are downregulated. Basal expression levels in tpm units are shown in the mock column. The fold change upon infection is shown in the EBOV and MARV columns. SAA1/2, CP are highly expressed in livers normally and also get highly up regulated by the filovirus (MARV more than EBOV). ORM2, MGST2 are highly upregulated, but from a low basal expression level. CRP, used as a marker for acute phase response in humans, does not appear to be expressed in these bats and might be absent in bats altogether. TF is highly expressed in all samples, but does not react to filoviral infection, while TTR is not expressed in any of the samples. There is similar inflammation in the liver upon both MARV and EBOV infection, despite the lack of viral transcripts in the liver of EBOV infected animals.\* signifies the bat gene is divergent from its human homolog.